

# Mitogen activated protein kinase at the nuclear pore complex

Randolph S. Faustino<sup>a</sup>, Thane G. Maddaford<sup>a</sup>, Grant N. Pierce<sup>a, b, \*</sup>

<sup>a</sup> *Institute of Cardiovascular Sciences, St Boniface Hospital Research Centre, and Department of Physiology, Faculty of Medicine, University of Manitoba, Winnipeg, Canada*

<sup>b</sup> *Faculty of Pharmacy, University of Manitoba, Winnipeg, Canada*

*Received: January 7, 2010; Accepted: March 19, 2010*

## Abstract

Mitogen activated protein (MAP) kinases control eukaryotic proliferation, and import of kinases into the nucleus through the nuclear pore complex (NPC) can influence gene expression to affect cellular growth, cell viability and homeostatic function. The NPC is a critical regulatory checkpoint for nucleocytoplasmic traffic that regulates gene expression and cell growth, and MAP kinases may be physically associated with the NPC to modulate transport. In the present study, highly enriched NPC fractions were isolated and investigated for associated kinases and/or activity. Endogenous kinase activity was identified within the NPC fraction, which phosphorylated a 30 kD nuclear pore protein. Phosphomodification of this nucleoporin, here termed Nup30, was inhibited by apigenin and PD-98059, two MAP kinase antagonists as well as with SB-202190, a pharmacological blocker of p38. Furthermore, high throughput profiling of enriched NPCs revealed constitutive presence of all members of the MAP kinase family, extracellular regulated kinases (ERK), p38 and Jun N-terminal kinase. The NPC thus contains a spectrum of associated MAP kinases that suggests an intimate role for ERK and p38 in regulation of nuclear pore function.

**Keywords:** nuclear pore complex • nuclear transport • phosphorylation • kinase • ERK-1/2 • smooth muscle cell

## Introduction

Mitogen activated protein (MAP) kinases are a group of enzymes involved in proliferative eukaryotic signalling. They are a diverse family, but can be classified into three main branches: the extracellular regulated kinases (ERK), p38 and Jun N-terminal kinase (JNK) families [1]. MAP kinases play a role in cellular development, differentiation and proliferation [2–5], regeneration/wound healing [6–8], adaptive and compensatory cell growth [9–11] and cellular apoptosis [12]. Proliferative signalling cascades are initiated by growth factors or stress stimuli that activate an upstream kinase, the first in a series of several kinases in a mitogen activated protein kinase (MAPK) activating module [1]. Elucidation of the role of the MAP kinase cascade in signal transduction pathways and the identification of targets for MAPK activity is thus critical to enhancement of knowledge regarding cell growth, death and regeneration.

Nucleocytoplasmic trafficking is an essential process required for normal cell growth, viability and function, and is a complex hierarchical process involving soluble cytosolic components and

membrane-bound machinery [13]. Molecules that shuttle between cytosolic and nucleoplasmic compartments must traverse outer and inner nuclear membranes of the nuclear envelope to reach their functional compartment. A large multiproteinaceous structure, the nuclear pore complex (NPC), spans both membranes of the nuclear envelope and serves as the gateway through which these molecules transit [14–23].

NPCs are dynamic and highly regulated structures that demonstrate robust evolutionary conservation across various species [20]. Mammalian NPCs are estimated to be roughly 125 MDa in mass and composed of hundreds of nuclear pore proteins called nucleoporins [20]. At its core, it is composed of eight multimeric subunits arranged in a distinctive barrel-like shape with a central channel ~9–11 nm in diameter [24, 25]. The nuclear pore is a highly dynamic structure that changes chronically and acutely in response to a variety of stimuli [26–29]. For example, NPC density responds to metabolic and physical stimuli [30–32]. Acutely, the central pore dilates to accommodate larger cargoes in transit [33, 34]. Furthermore, a calcium-sensitive mechanism responsible for pore closing and opening [35, 36] supports the notion that the NPC is dynamically regulated by calcium fluxes in and around the nucleus [35–37]. In addition to the main central channel [38, 39], peripheral channels exist which are suggested to permit the flow of various small molecules and ions [16, 40].

\*Correspondence to: Grant N. PIERCE, Ph. D., Institute of Cardiovascular Sciences, St Boniface Hospital Research Centre, 351 Tache Ave., Winnipeg, Manitoba R2H 2A6, Canada.  
Tel.: 204-235-3206  
Fax: 204-235-0793  
E-mail: gpierce@sbrcc

It is reasonable to suggest that a significant relationship may exist between MAP kinase signalling and nucleocytoplasmic trafficking as it relates to cellular growth, viability and function. The role of MAP kinases with respect to nuclear trafficking has concentrated primarily on phosphorylation of amino acids adjacent to nuclear transport (import or export) signals in proteins being moved through the pore [41, 42]. Physiologically relevant MAP kinase mediated phosphorylation may also occur within the NPC [41–46]. This study describes the MAP kinase profile of an enriched NPC fraction and provides biochemical evidence for a close physical localization of MAP kinases with the NPC, which suggests a novel property of the NPC as a coordinating hub for MAP kinase activity.

## Materials and methods

### Smooth muscle cell isolation and culture

Smooth muscle cells were obtained from aortic vessel explants, according to established protocols [47–49]. Cells were maintained in quiescence, or stimulated to proliferate with the addition of 5% foetal bovine serum to the medium, as previously described [50, 51].

### Immunocytochemistry

Cells and nuclear import mix were prepared as described for the nuclear import assay, with minor modifications. For these experiments, ALEXA™-bovine serum (Molecular Probes/Life Technologies, Burlington, Canada) albumin–nuclear localization signal (NLS) substrate was not included. Immunofluorescent reactions were detected as previously described, with the following modifications. After cells were fixed with 3.7% paraformaldehyde, they were incubated in blocking buffer (1× PBS [phosphate-buffered saline], 2% skim milk, 0.1% Triton X-100) for 30 min. at room temperature. Cover slips were washed 3× with wash buffer (1× PBS, 2% skim milk) and inverted on 50 µl of wash buffer containing a 1:100 dilution of primary antibody in a Parafilm-lined box. Cover slips were incubated for 1 hr at room temperature, washed 3× and then incubated with a 1:1000 dilution of ALEXA-conjugated goat antimouse secondary antibody for 1 hr. Cover slips were rinsed with 1× PBS and mounted on glass slides using Fluorsave (Fluorsave Calbiochem, San Diego, CA, USA). After drying, cells were visualized using a 63× objective lens and a 488 nm filter block on a Zeiss Axioskop 2 MOT microscope (Carl Zeiss Canada Ltd, Toronto, ON, Canada). Images were captured using a Zeiss Axiocam and pseudo-coloured using Axiovision Viewer v3.0 (Carl Zeiss).

### Isolation of hepatic tissue nuclei and an enriched nuclear pore complex fraction

Nuclei were isolated from hepatic tissue obtained from Sprague-Dawley rats as described in detail by Gilchrist and colleagues [52]. The nuclei were stored at –80°C for later use in the isolation of the NPC. The NPC-enriched fraction was isolated by the method of Berrios [53]. Briefly, nuclei from rat

liver were pelleted and resuspended in a tube with nuclease digestion buffer [10 mM triethanolamine (TEA), 0.23 M sucrose, 0.1 mM MgCl<sub>2</sub>, pH 8.5] containing ~1 µg/ml of DNase I and RNase A. The tube was then incubated at 37°C for 30 min., with occasional shaking. The suspension was centrifuged for 10 min. at 1000 × *g* and the supernatant discarded. The pellet was resuspended in 0.9 volumes of nuclear extraction buffer (10 mM TEA, 0.29 M sucrose, 0.1 mM MgCl<sub>2</sub>, pH 7.5). One volume is defined by digested nuclear pellets, where the volume of one pellet is equivalent to one volume. After resuspension, 0.1 volume of cold 20% Triton X-100 (v/v) was added and incubated on ice for 10 min. This mixture was re-centrifuged for 10 min. at 1000 × *g* and the supernatant discarded. The remaining pellet was resuspended in five volumes of nuclear extraction buffer and an equal volume of 2.0 M NaCl. This mixture remained on ice for 10 min., and was then centrifuged for 10 min. at 10,000 × *g*. The supernatant was discarded and the previous step was repeated. The final pellet, containing the enriched NPC fraction was resuspended in 500 µl of 250 mM STM [250 mM sucrose, 50 mM tris(hydroxymethyl)aminomethane (TRIS), 5 mM MgCl<sub>2</sub>, pH 7.5], snap frozen in liquid N<sub>2</sub> and stored at –80°C. Protein concentrations of nuclear and nuclear pore fractions were determined using the DC Protein Assay Kit (Bio-Rad Laboratories, Hercules, CA, USA).

### Immunoblotting

SDS-PAGE was performed as described above on both the precipitated and non-precipitated NPC fractions. After completing electrophoresis, the gel was placed in Towbin's buffer (25 mM TRIS-OH, 192 mM glycine, 20% (v/v) methanol, pH 8.3) and allowed to soak for 15–20 min. Proteins were then transferred onto a nitrocellulose membrane at 50 V for 45 min. After the transfer was completed, the membrane was placed in 10% blocking buffer (10% (w/v) skim milk powder, 0.1% (v/v) Tween-20, 1× PBS) for 1 hr at room temperature with shaking. Blocking buffer was then decanted and the membrane was washed every 10 min. for 30 min. with wash buffer (1× PBS, 0.1% (v/v) Tween-20). Following transfer, the nitrocellulose membrane was incubated in Ponceau S stain for 10 min. to visualize proteins and assess transfer efficiency. Ponceau S was rinsed off the membrane with several changes of PBS and the membrane was transferred to wash solution containing primary antibody for immunoblotting.

The membrane was incubated with primary antibody diluted in 1% blocking buffer (1% (w/v) skim milk powder, 0.1% (v/v) Tween-20, 1× PBS) for 1 hr at room temperature with constant shaking. After incubation, the primary antibody was poured off and the membrane was washed again for 30 min. every 10 min. A goat antimouse horseradish peroxidase (HRP) conjugate was the secondary antibody used in this experiment and was added to the membrane at a dilution of 1:20,000 in 1% blocking buffer and incubated for 1 hr at room temperature with shaking. The membrane was washed as mentioned earlier and then incubated for 15 min. with the Pierce SuperSignal Substrate Working Solution (Thermo Fisher Scientific, Rockford, IL, USA). The nitrocellulose was then placed in a protective plastic sheet and exposed to film for 60 sec. to determine working exposure. Primary antibodies used and their dilutions: mAb414 (1:10,000), anti-p38 (1:10,000), anti-lamin A/C (1:10,000), anti-lamin B<sub>1</sub> (1:10,000) and anti-karyopherin α (1:1000). For immunoblots using anti-karyopherin α, all buffers and antibody dilutions were done using 1× TRIS buffer saline (TBS) (10 mM TRIS, 100 mM NaCl, 0.1% (v/v) Tween-20, pH 7.5), instead of PBS solutions as noted above.

For high throughput analysis of kinase and phosphatase content within the enriched NPC fraction, aliquots (1 mg/ml) were prepared for submission to, and analysis by, Kinexus ([www.kinexus.ca](http://www.kinexus.ca)), a systems proteomics company specializing in high throughput assessment of phosphoproteomes.

## Immunoprecipitation

The NPC was immunodepleted of lamins by immunoprecipitation. It was carried out as previously described [54]. The NPC/lamin enriched fraction was pre-cleared by incubating 1.0  $\mu\text{g}$  of normal mouse serum IgG and 20  $\mu\text{l}$  of protein G-agarose overnight at 4°C with end-over-end rotation. Samples were then centrifuged at  $1000 \times g$  for 5 min. The supernatant was transferred to a new tube and 2  $\mu\text{g}$  of anti-lamin A/C (Santa Cruz Biotechnology, Inc., Santa Cruz, CA, USA) and 10  $\mu\text{l}$  each of protein A and protein G agarose conjugate was added. The fraction was incubated overnight at 4°C with end-over-end rotation. The following day, the tube was centrifuged at  $1000 \times g$  for 5 min. to sediment the antibodies. Again, the supernatant was transferred to a new tube and the immunoprecipitation step was repeated, this time using 5  $\mu\text{l}$  of a 1 mg/ml solution of anti-lamin B<sub>1</sub> antibody. After overnight incubation, the tube was re-centrifuged for 5 min. at  $1000 \times g$  to pellet out the anti-lamin B<sub>1</sub>. All pellets were saved in addition to the final lamin-precipitated NPC fraction.

## Enzyme marker assays

Enzyme marker assays were used to determine membrane contamination from plasmalemma, endoplasmic reticulum and mitochondrial sources in the nuclear fraction. Purified samples of plasmalemma, endoplasmic reticulum/sarcoplasmic reticulum and mitochondria were used as comparative controls.  $\text{K}^+$ -pNPPase activity can be used to assay the degree of sarcolemmal contamination [55].  $\text{K}^+$ -pNPPase activity was measured as described in detail previously [52, 53]. Mannose-6-phosphatase activity derived from the endoplasmic reticulum was assayed as previously described [52]. Mitochondrial contamination was assessed using the succinic dehydrogenase assay as described previously [55].

## Phosphorylation assay and SDS-PAGE

NPC phosphorylation was investigated using a phosphorylation assay described previously [54] with minor modifications. Here, 40  $\mu\text{g}$  of sample was incubated with or without (1  $\mu\text{g}/\text{ml}$ ) ERK-2, JNK or p38 in phosphorylation buffer [40 mM 4-(2-hydroxyethyl)-1-piperazineethanesulfonic acid (HEPES), 10 mM  $\text{MgCl}_2$ , 1 mM dithiothreitol (DTT), pH 7.5] and 2.0  $\mu\text{Ci}$  of  $^{32}\text{P}$  for a total volume of 50  $\mu\text{l}$ . To investigate endogenous phosphorylation, samples were treated with or without kinase antagonists. Inhibitors: 1  $\mu\text{M}$  autocalmitide-2 related inhibitory peptide (AIP) and 1  $\mu\text{M}$  CaM kinase inhibitory peptide (CKI), specific and potent inhibitors of calmodulin-dependent protein kinase 2; 20  $\mu\text{M}$  PD-98059, a selective and cell permeable inhibitor of MAP kinase kinase (MEK), the activating kinase directly upstream of ERK [56]; 0–100  $\mu\text{M}$  apigenin, an inhibitor of the Ras/Raf/MEK/ERK cascade [57] and 0–1000 nM SB-202190, a potent antagonist of the p38 signalling pathway [58]. The concentrations of each inhibitor used were selected according to  $\text{IC}_{50}$  values reported in the literature, to guarantee pharmacological blockade without toxic effect. The reaction mixture incubated at room temperature for 1 hr and stopped by addition of an equivalent amount of 2 $\times$  sample buffer. Samples were boiled for 5 min. at 95°C, then loaded onto a 4–15% gradient gel, or alternatively onto a 10% minigel, for SDS-PAGE. Electrophoresis conditions: 60 mA, 550V for ~3–4 hrs (gradient gel) or 30 mA for 90 min. (minigel). Coomassie Brilliant Blue stained protein bands and gels were dried then exposed to KODAK X-OMAT film (Kodak, Toronto, ON, Canada) overnight at –80°C. Film was developed the following day. Phosphoimaging and densitometry analysis was performed using the molecular dynamics phosphoimager.

## Results

### Differential phosphodistribution before and after growth stimulus

Vascular smooth muscle cells localized the MAP kinase ERK according to proliferative state. Growth stimulus induced general nuclear accumulation of ERK (Fig. 1A, B) and its phosphorylated, activated form (pERK) (Fig. 1C, D). Though ERK distribution was diffuse throughout the cytoplasm and concentrated within the nucleus during proliferation, activated ERK (pERK) exhibited distinct filament-like distribution independent of proliferative state (Fig. 1C, D).

ERK is a serine/threonine kinase, and investigation of phosphoserine and phosphothreonine distribution during quiescent and proliferative conditions revealed a concentrated nuclear localization during periods of no growth for both phosphoresidues (Fig. 2A, C). Nuclear prominence of phosphoserine was maintained after growth stimulus (Fig. 2B); however, phosphothreonine staining accumulated throughout the cytoplasm under proliferative conditions, without preferential nuclear accumulation (Fig. 2D). Moreover, analysis of phosphorylated serine and threonine residues demonstrated intense, punctate nuclear envelope staining that prompted assessment of the NPC phosphorylation profile.

### Nuclear pore complex enrichment

To investigate NPC-resident phosphosubstrates, NPC-rich fractions were purified from isolated nuclei. A scheme for NPC enrichment in the present study outlines consecutive fractionation steps (Fig. 3A) that illustrate progressive purification. Sequential centrifugation and saline washes enriched nucleoporin content with concomitant removal of contaminants (Fig. 3B). Biochemical enzyme assays, to confirm removal of contaminating plasmalemma, mitochondria and endoplasmic reticulum membranes demonstrated negligible contamination (data not shown). Lamins are highly phosphorylated nuclear proteins between 60 and 70 kD that co-purify with enriched NPCs [59, 60]. Here, lamins A/C and B1 were immunodepleted to further enrich the NPC fraction (Fig. 3C).

### Endogenous kinase activity within the enriched nuclear pore complex fraction

Nuclear distribution of ERK and putative (phospho)serine/threonine-containing ERK substrates suggested co-purification of kinases with NPCs. To investigate kinase content of highly purified NPCs, a high throughput Kinetworks Protein Kinase Screen that profiles kinase and phosphatase content, revealed enrichment of ERK, p38, JNK, death-associated protein kinase 3 (ZIP), Cdk7 and protein kinase C (PKC) kinases, as well as protein phosphatases PP1, PP5, MAPK phosphatase 1, PP2A and PP2X (Table 1).

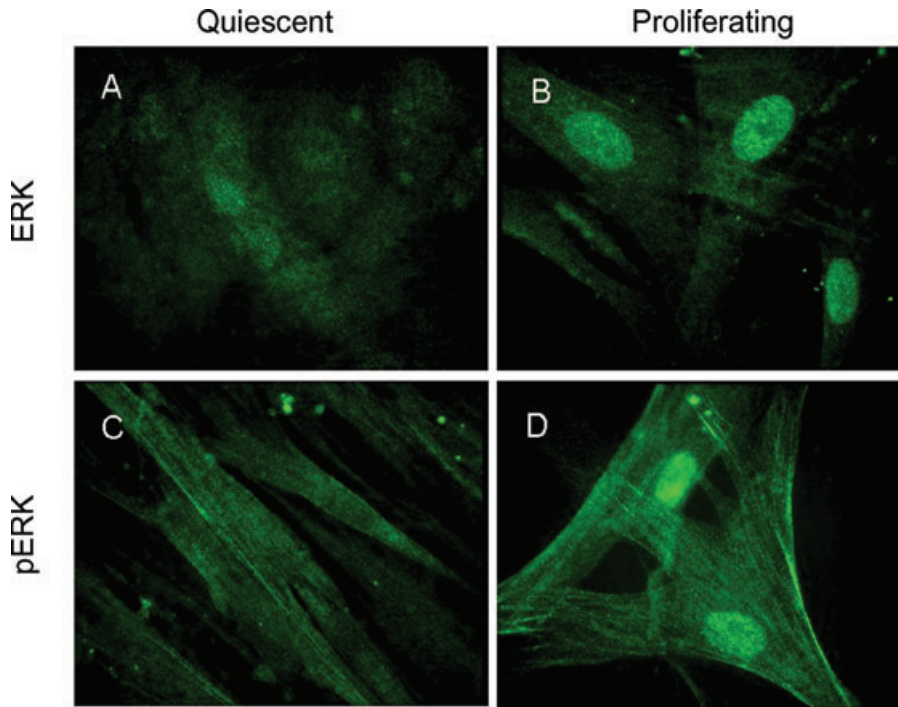


**Fig. 1** ERK distribution before and after growth stimulation. Cultured smooth muscle cells were stained to visualize the distribution of MAP kinases within quiescent and proliferating smooth muscle cell. **(A)** Quiescent cells exhibited diffuse, cytosolic localization of non-activated ERK-2 that was concentrated within the nucleus in proliferating cells **(B)**. Activated ERK-2 demonstrated a distribution pattern reminiscent of actin staining in quiescent cells **(C)** and with robust nuclear localization upon proliferation **(D)**. Images representative of results obtained from sample size of  $n = 3$ .

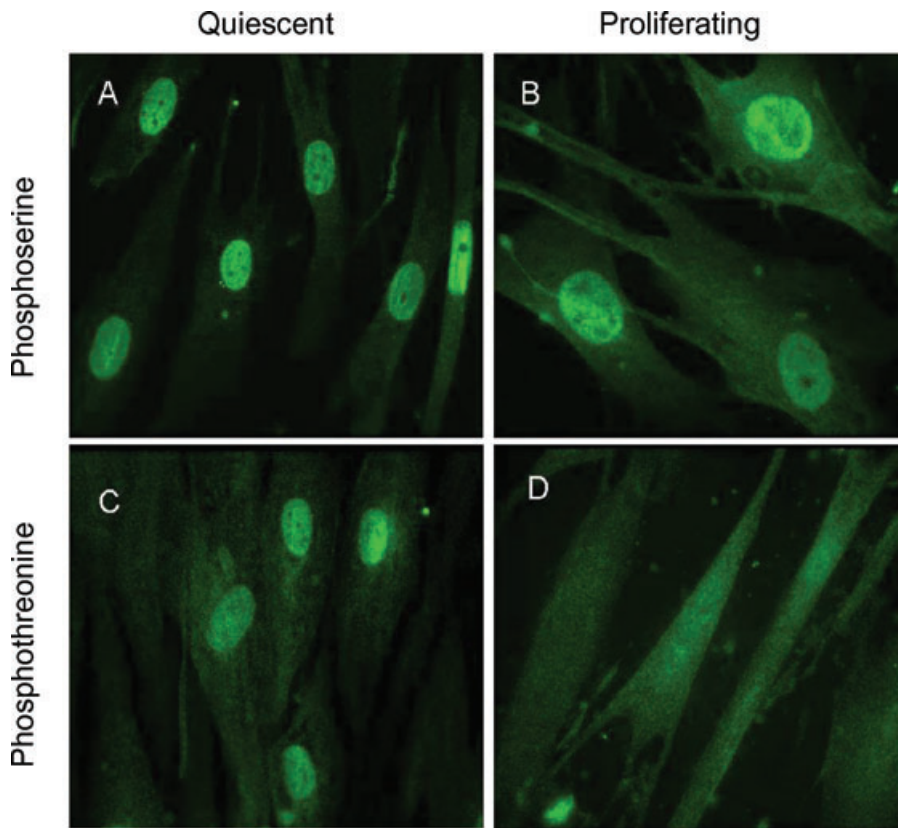


**Fig. 2** Broad phosphoprofile of putative ERK substrates in quiescent and proliferating smooth muscle cells. Smooth muscle cells were stained using antibodies against phosphoserine and phosphothreonine. **(A)** In quiescent cells, phosphoserine containing proteins localized primarily to the nucleus with faint cytosolic staining. **(B)** Proliferation caused moderate increases in cytosolic distribution of phosphoserine, but maintained nuclear presence. **(C)** Quiescent cells stained for phosphothreonine diffuse throughout cytosolic and nuclear compartments, but exhibits even distribution among both in proliferating cells **(D)**. Images representative of results obtained from sample size of  $n = 3$ .

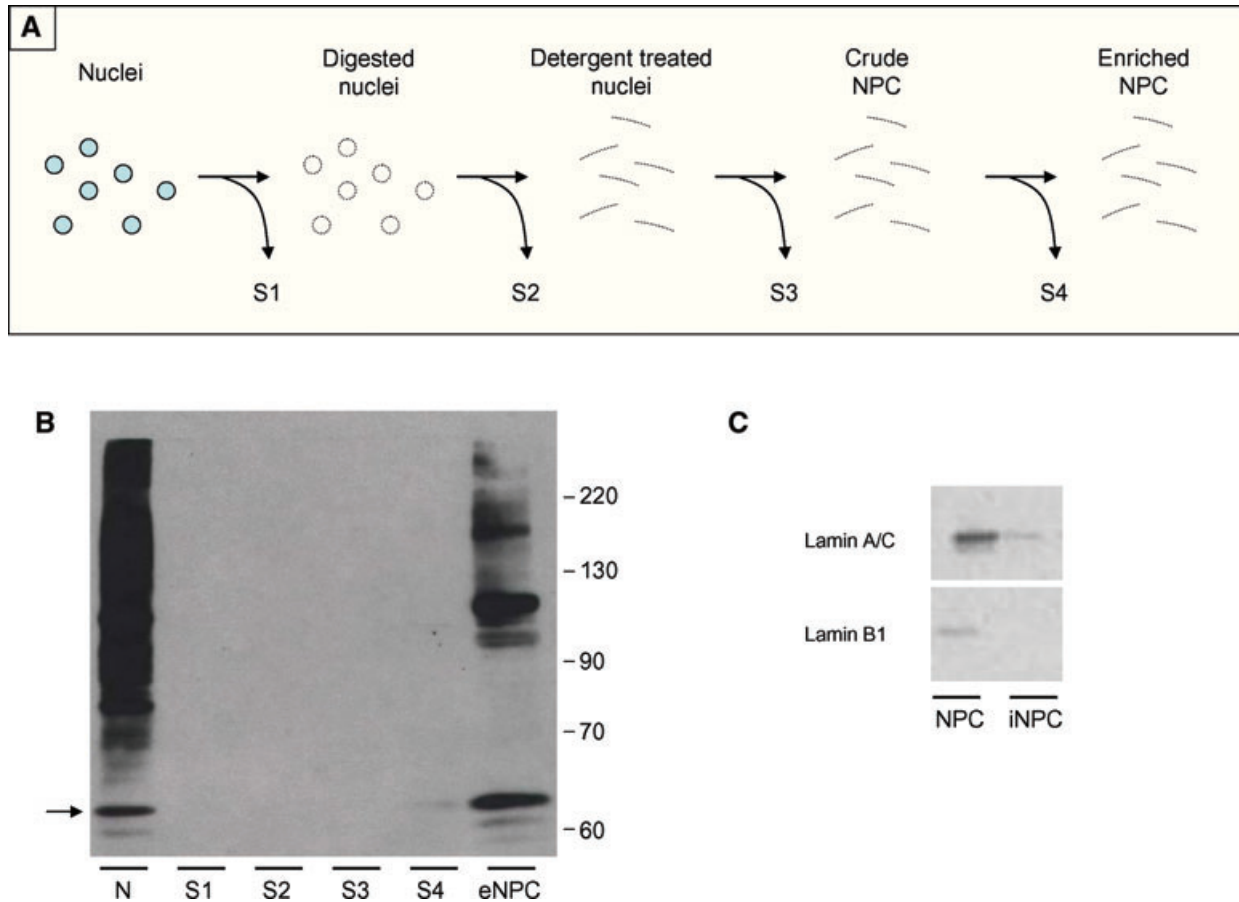


**Fig. 3** Isolation of a purified NPC fraction. **(A)** NPC isolation workflow, illustrating sequential enrichment procedure. S1–S4 indicate supernatant fractions. **(B)** Fractions from the NPC isolation procedure were loaded onto SDS-PAGE (50  $\mu$ g per lane) and immunoblotted using mAb414. Crude nuclei (N) show staining of p62 (arrow), a nucleoporin recognized by mAb414, with subsequent enrichment in the final NPC-rich fraction (eNPC). Lane assignments: N: crude nuclei; S1: supernatant from nuclease digested nuclei; S2: supernatant from detergent extracted nuclei; S3: supernatant from first salt wash; S4: supernatant from second salt wash; eNPC: purified NPC/lamina fraction. Numbers to the right indicate molecular mass markers in kD. **(C)** Removal of lamins from NPC fraction. NPC fractions were immunodepleted of nuclear lamins prior to use in the phosphorylation assays. Illustrated are representative immunoblots of NPC fractions that were depleted, then probed for lamins A/C or B1. In both cases, lamins were effectively removed. Pre-immunodepletion samples were loaded on the right for comparison. NPC: nuclear pore complex; iNPC: immunodepleted NPC.

Kinases and phosphatases are essential phosphoregulatory components and the presence of these molecules within enriched NPC fractions suggested phosphorylation activity resident to the pore. Purified NPCs incubated with radiolabelled ATP demonstrated strong endogenous, time-dependent phosphorylation of a 30 kD protein (Fig. 4). As the NPC has been associated with calcium regulation [35], the possibility of endogenous calcium-dependent kinase activity was investigated. However, addition of  $\text{Ca}^{2+}$  or EGTA, a calcium chelator, did not affect phosphorylation profile of this nuclear pore protein, which we refer to as Nup30. However, apigenin and PD98059, two ERK antagonists, significantly diminished phosphorylation of Nup30, compared to phosphorylation of untreated controls. Specifically, apigenin inhibited

phosphorylation of Nup30 more than PD98059 (Fig. 5). Pharmacological inhibition with AIP and CKI did not affect Nup30 phosphorylation. Endogenous phosphorylation of Nup30 demonstrated dose-dependent antagonism in response to increasing concentrations of apigenin, with over 70% inhibition at 100  $\mu$ M, the highest levels used in the current study (Fig. 6).

ERK and p38 cascades represent well-studied proliferative signalling axes within the MAP kinase family [47, 50]. Activated p38 demonstrated nuclear speckling and diffuse cytoplasmic distribution while quiescent, and exhibited robust nuclear localization under proliferating conditions (Fig. 7A). Phosphorylation of Nup30 was sensitive to antagonism by SB202190, demonstrating 40% inhibition at maximal dosage (Fig. 7B).

**Table 1** Kinase and phosphatase content of enriched nuclear pore fractions

Kinases	Phosphatases
ERK	PP1 ( $\alpha$ , $\beta$ and $\gamma$ isoforms)
p38/MAPK14	PP5
JNK	DUSP1
ZIP/DAPK3	PP2A (A subunit)
Cdk7	PP2X (catalytic subunit)
PKC ( $\epsilon$ and $\zeta$ isoforms)	

Enriched NPCs were submitted to Kinexus for high throughput profiling to analyse kinases and phosphatases significantly associated with the purified fraction. All branches of the MAP kinase family (ERK, p38, and JNK) were represented, as well as ZIP, Cdk7 and PKC. DUSP1, and protein phosphatases 1, 2 and 5 were also detected.

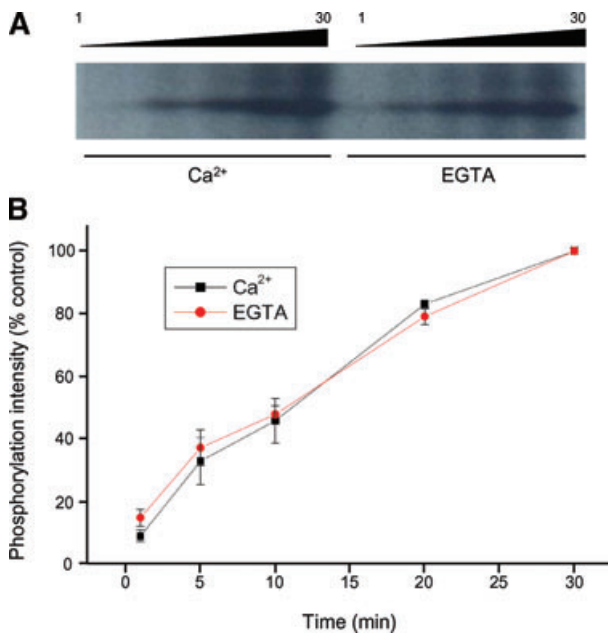


**Fig. 4** Calcium-independent endogenous phosphorylation of enriched NPC fraction. The purified NPC fraction was incubated in kinase reaction buffer in the presence or absence of 5 mM calcium for different times before stopping with 2% SDS. Typical reaction blots are shown in (A). Endogenous phosphorylation of a 30 kD protein within the purified NPC fraction does not show any calcium dependency. Incubation of the reaction mixture in the presence of 5 mM EGTA, a chelating agent, does not show any attenuation in phosphorylation after 30 min. The results from several independent experiments are shown in (B) ( $n = 4$ ).

## Discussion

NPCs are tightly regulated macromolecular features critical for control of nucleocytoplasmic trafficking essential to eukaryotic

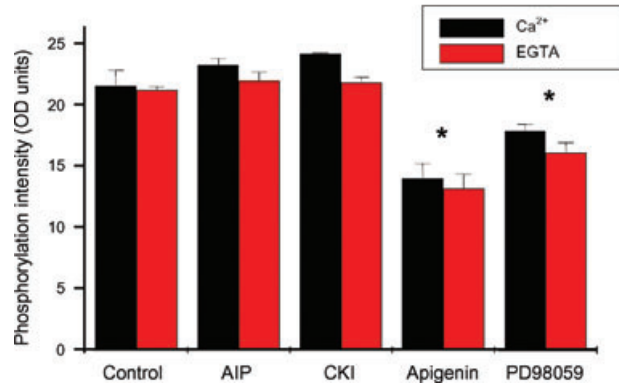
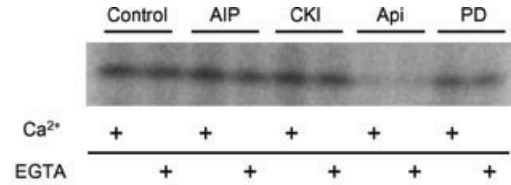


**Fig. 5** Endogenous phosphorylation antagonized by MAP kinase inhibitors. Various pharmacological antagonists were incubated with the final, purified NPC fraction in the presence and absence of EGTA. Endogenous phosphorylation of a protein within the NPC fraction was significantly inhibited by apigenin, a broad range MAP kinase inhibitor. Controls contained no inhibitor and consisted solely of purified NPCs. Inhibitors used – AIP (30 nM); CKI (40  $\mu$ M), apigenin (50  $\mu$ M), PD-98059 (40  $\mu$ M). Results representative of independent samples ( $n = 3$ ).

function. MAP kinase signalling governs cellular proliferation and constitutively shuttles between nuclear and cytoplasmic compartments, but association of MAP kinases with NPCs remains poorly characterized. Enrichment of NPCs enhanced samples for assessment of endogenous phosphoregulation, which revealed intimate association of MAP kinases with accompanying endogenous kinase activity. The presence of phosphoregulatory molecules and resident phosphosubstrates at the NPC, therefore, suggests a capacity for dynamic coordination of MAP kinase activity.

Previous studies have demonstrated presence of substrates phosphorylated by mitotically regulated kinases [44, 45] as well as NPC regulation by protein kinase A (PKA) and PKC [46]. Here, an endogenously phosphorylated protein of ~30 kD (Nup30) was identified as an ERK substrate. This was not verified, however, by purifying the Nup30 protein from the NPC and exposing it to exogenous ERK activity. Nonetheless, the presence of MAP kinases and their phosphosubstrates within the NPC argue in favour of a functional contribution. Kinase-dependent phosphorylation of channels alters channel activity [61–63] and MAP kinase activation can modulate protein transport into the nucleus through the NPC [47–49, 64]. A recent phosphoproteomics study demonstrated that ERK MAPK-mediated phosphorylation of a nucleoporin

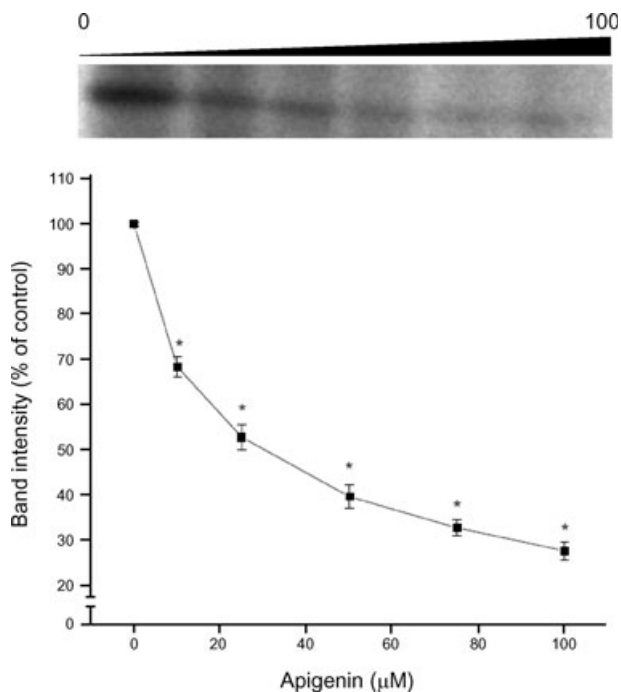


**Fig. 6** Dose-dependent inhibition of endogenous MAP kinase activity. The 30 kD protein within the NPC fraction was inhibited in a concentration-dependent manner using increasing amounts of apigenin. Molecular weight is given on the side in kD. Below: Graphical analysis of a number of experiments ( $n = 3$ ) reveals potent inhibition of endogenous kinase activity with increasing doses. Data were reported as mean  $\pm$  S.E.M. \* $P < 0.05$  versus control. Controls were taken to be band intensity of the protein in the absence of apigenin.

can inhibit nuclear transport of importin- $\beta$  [65]. Indeed, ERK substrates appear to be a constitutive feature of the nuclear pore [66].

No endogenous CaM kinase activity was observed with the NPC fraction. Immunological analysis of the nuclear pore fraction failed to detect any endogenous CaM kinases (data not shown), in line with lack of observable  $\text{Ca}^{2+}$ - or EGTA-sensitive phosphosubstrates within the pore. High throughput profiling of kinase and phosphatase components in enriched NPC fractions confirmed absence of intimately associated CaM kinases. Although  $\text{Ca}^{2+}$  handling enzymes and  $\text{Ca}^{2+}$  binding proteins reside within the nucleus and the nuclear envelope [67, 68], and the NPC is sensitive to  $\text{Ca}^{2+}$  flux [27, 35, 36, 69], the lack of endogenous CaM kinases at the NPC suggests that transiently, rather than innately, associated CaM kinases may participate in nuclear pore function. Furthermore, lack of CaM kinase association with the NPC suggests that association of ERK kinases with the NPC is not a random event but a specific interaction.

ERK and p38 are a class of serine/threonine kinases that showed robust nuclear localization as a function of proliferation. Increased nuclear translocation of MAP kinases is necessary for initiation and propagation of proliferative signalling [70].

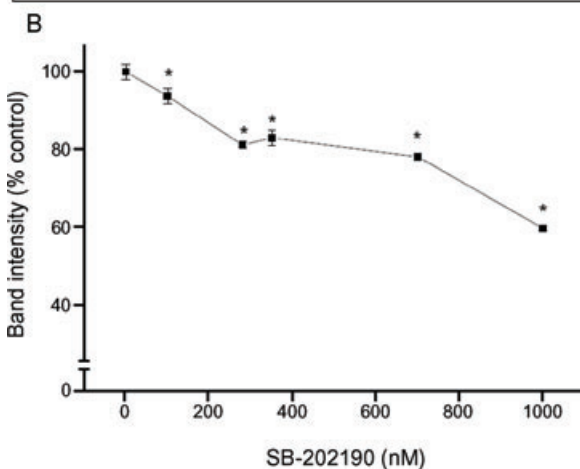
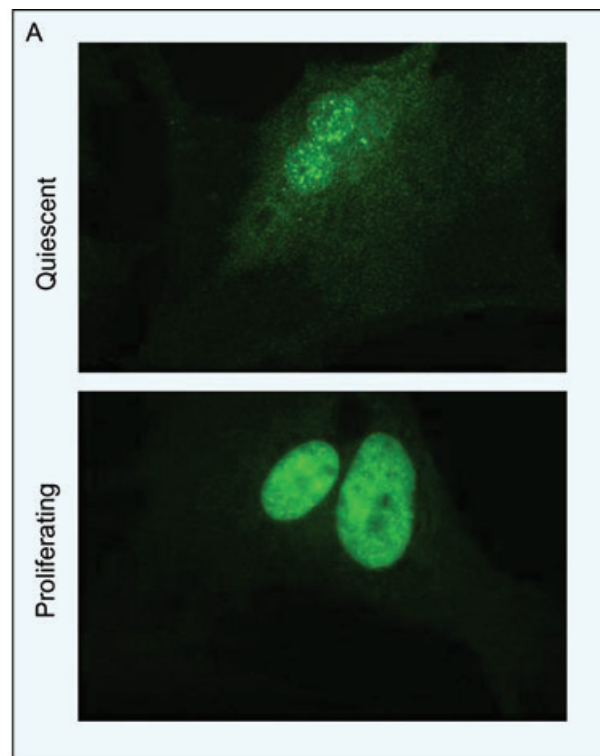


**Fig. 7** Involvement of p38 MAP kinase. (A) Activated p38 showed diffuse cytosolic, and speckled nuclear, staining in quiescent cells (upper panel) which localized the nucleus in proliferating cells (lower panel). (B) Dose-dependent inhibition of endogenous NPC phosphorylation by SB-202190. Incubation of phosphorylation reaction mixture with SB-202190 attenuated endogenous phosphorylation of the 30 kD band in the NPC fraction. Data were reported as mean  $\pm$  S.E.M. from several experiments ( $n = 3$ ). \* $P < 0.05$  versus control. Controls were taken to be phosphorylation intensity of protein in the absence of SB-202190.

Constitutive nuclear distribution of substrates that harbour phosphoserine and phosphothreonine residues under conditions of

quiescence complement nuclear MAP kinase residency. The altered distribution of phosphosubstrates under proliferative conditions may indicate increased contribution of phosphatase activity, or alternatively represent proteins that serve as substrates for kinases other than ERK and p38.

ERK activity is intimately associated with nuclear processes and regulates phosphosubstrates that shuttle between nuclear and cytoplasmic components [70, 71]. Accumulation of ERK within the nucleus is a hallmark of growth stimulation [72, 73], and ERK substrates within the nucleus and nuclear membrane are critical for normal cell growth. The distribution of activated ERK along actin filaments is supported by the observation that caldesmon mediates ERK/actin association in order to collectively stabilize cytoskeletal architecture. Furthermore, in smooth muscle cells, the ERK/caldesmon signalling cascade is critical for regulation of contractility [74, 75].

ERK activity phosphorylated Nup30, a novel phosphosubstrate identified here within enriched NPC fractions. Its molecular weight may represent a stable histone phosphostate, as unmodified histones migrate at molecular weights between 10 and 30 kD, although only the 17 kD histone H3 has been reported as an ERK substrate [76]. Full identity of Nup30 remains intriguing and thus warrants further consideration.

Sensitivity to SB-202190 suggested influence of p38 kinase signalling in addition to the ERK cascade inhibited by apigenin and PD-98059, suggesting influence of other members of the MAP kinase family. Here, though still significant, antagonism of Nup30 phosphorylation by SB-202190 was less dramatic than that of apigenin. The plateau observed within the dose–response plot of SB-202190 may indicate differential antagonism of p38 $\alpha$  and p38 $\beta$ , as higher concentrations of SB-202190 have been reported to inhibit the latter p38 $\beta$ . Furthermore, SB-202190 does not inhibit

members of the ERK signalling cascade, which may account for the greater degree of Nup30 phosphorylation observed with maximal dosage of SB-202190 used in this study.

In summary, our data suggest that MAP kinase signalling is a physiologically relevant process coordinated at the NPC. The presence of intimately associated ERK and p38, as well as a pharmacologically sensitive substrate, Nup30, suggest integration of MAP kinase into overall NPC function. This is complemented by high throughput identification of several species of NPC-associated phosphatases which are critical functional counterparts to kinase signalling, and essential to local phosphorylation control [77]. Consideration of the NPC as a coordinating hub for MAP kinase activity is in line with observations that chromatin arrangement and gene regulation are mediated by the pore [78, 79]. Dynamic MAP kinase phosphoregulation at the NPC expands functional role of the pore, and provides support for a growing body of evidence that MAPK activation is critical to nucleocytoplasmic trafficking.

## Acknowledgements

This work was supported by a grant from the Canadian Institutes for Health Research and infrastructural support from St. Boniface Hospital & Research Foundation.

## Conflict of interest

The authors confirm that there are no conflicts of interest.

## References

1. **Pearson G, Robinson F, Gibson TB, et al.** Mitogen-activated protein (MAP) kinase pathways: regulation and physiological functions. *Endocr Rev.* 2001; 22: 153–83.
2. **Buehr M, Smith A.** Genesis of embryonic stem cells. *Philos Trans R Soc Lond B Biol Sci.* 2003; 358: 1397–402.
3. **Yao Y, Li W, Wu J, et al.** Extracellular signal-regulated kinase 2 is necessary for mesoderm differentiation. *Proc Natl Acad Sci USA.* 2003; 100: 12759–64.
4. **Burdon T, Smith A, Savatier P.** Signalling, cell cycle and pluripotency in embryonic stem cells. *Trends Cell Biol.* 2002; 12: 432–8.
5. **Jirmanova L, Afanassieff M, Gobert-Gosse S, et al.** Differential contributions of ERK and PI3-kinase to the regulation of cyclin D1 expression and to the control of the G1/S transition in mouse embryonic stem cells. *Oncogene.* 2002; 21: 5515–28.
6. **Kook H, Itoh H, Choi BS, et al.** Physiological concentration of atrial natriuretic peptide induces endothelial regeneration *in vitro*. *Am J Physiol Heart Circ Physiol.* 2003; 284: H1388–97.
7. **Sharma G-D, He J, Bazan HEP.** p38 and ERK1/2 coordinate cellular migration and proliferation in epithelial wound healing. *J Biol Chem.* 2003; 278: 21989–97.
8. **Yates S, Rayner TE.** Transcription factor activation in response to cutaneous injury: role of AP-1 in reepithelialization. *Wound Repair Regen.* 2002; 10: 5–15.
9. **Bueno OF, Molkentin JD.** Involvement of extracellular signal-related kinases 1/2 in cardiac hypertrophy and cell death. *Circ Res.* 2002; 91: 776–81.
10. **Nader GA, Esser KA.** Intracellular signaling specificity in skeletal muscle in response to different modes of exercises. *J Appl Physiol.* 2001; 90: 1936–42.
11. **Michel MC, Li Y, Heusch G.** Mitogen-activated protein kinases in the heart. *Arch Pharmacol.* 2001; 363: 245–66.
12. **Wada T, Peninger JM.** Mitogen-activated protein kinases in apoptosis regulation. *Oncogene.* 2004; 23: 2838–49.
13. **Terry LJ, Shows EB, Wente SR.** Crossing the nuclear envelope: hierarchical regulation of nucleocytoplasmic transport. *Science.* 2007; 318: 1412–6.
14. **Forbes DJ.** Structure and function of the nuclear pore complex. *Annu Rev Cell Biol.* 1992; 8.
15. **Hinshaw JE.** Architecture of the nuclear pore complex and its involvement in

- nucleocytoplasmic transport. *Biochem Pharmacol.* 1994; 47: 15–20.
16. **Hinshaw JE, Carragher BO, Milligan RA.** Architecture and design of the nuclear pore complex. *Cell.* 1992; 69: 1133–41.
  17. **Panté N, Aebi U.** The nuclear pore complex. *J Cell Biol.* 1993; 122: 977–84.
  18. **Panté N, Aebi U.** Exploring nuclear pore complex structure and function in molecular detail. *J Cell Sci.* 1995; 19: 1–11.
  19. **Panté N, Aebi U.** Molecular dissection of the nuclear pore complex. *Crit Rev Biochem Mol Biol.* 1996; 31: 153–99.
  20. **Adam SA.** The nuclear pore complex. *Genome Biol.* 2001; 2: 1–6.
  21. **Miller M, Park MK, Hanover JA.** Nuclear pore complex: structure, function, and regulation. *Physiol Rev.* 1991; 71: 909–49.
  22. **Ryan KJ, Wente SR.** The nuclear pore complex: a protein machine bridging the nucleus and cytoplasm. *Curr Opin Cell Biol.* 2000; 12: 361–71.
  23. **Rout MP, Aitchison JD, Suprapto A, et al.** The yeast nuclear pore complex: composition, architecture, and transport mechanism. *J Cell Biol.* 2000; 148: 635–51.
  24. **Danker T, Oberleithner H.** Nuclear pore function viewed with atomic force microscopy. *Pflugers Arch.* 2000; 439: 671–81.
  25. **Panté N, Kann M.** Nuclear pore complex is able to transport macromolecules with diameters of ~39 nm. *Mol Biol Cell.* 2002; 13: 425–34.
  26. **Moore-Nichols D, Arnott A, Dunn RC.** Regulation of nuclear pore complex conformation by IP<sub>3</sub> receptor activation. *Biophys J.* 2002; 83: 1421–8.
  27. **Perez-Terzic C, Gacy AM, Bortolon R, et al.** Structural plasticity of the cardiac nuclear pore complex in response to regulators of nuclear import. *Circ Res.* 1999; 84: 1292–301.
  28. **Goldberg MW, Rutherford SA, Hughes M, et al.** Ran alters nuclear pore complex conformation. *J Mol Biol.* 2000; 300: 519–29.
  29. **Stoffler D, Goldie KN, Feja B, et al.** Calcium-mediated structural changes of native nuclear pore complexes monitored by time-lapse atomic force microscopy. *J Mol Biol.* 1999; 287: 741–52.
  30. **Maul GD, Deaven L.** Quantitative determination of nuclear pore complexes in cycling cells with differing DNA content. *J Cell Biol.* 1977; 73: 748–60.
  31. **Maul GG, Deaven LL, Freed JJ, et al.** Investigation of the determinants of nuclear pore number. *Cytogenet Cell Genet.* 1980; 26: 175–90.
  32. **Maul HM, Hsu BYL, Borun TM, et al.** Effect of metabolic inhibitors on nuclear pore formation during the HeLa S<sub>3</sub> cycle. *J Cell Biol.* 1973; 59: 669–76.
  33. **Feldherr C, Akin D, Moore MS.** The nuclear import factor p10 regulates the functional size of the nuclear pore complex during oogenesis. *J Cell Sci.* 1998; 111: 1889–96.
  34. **Feldherr CM, Akin D, Cohen RJ.** Regulation of functional nuclear pore size in fibroblasts. *J Cell Sci.* 2001; 114: 4621–7.
  35. **Perez-Terzic C, Jaconi M, Clapham DE.** Nuclear calcium and the regulation of the nuclear pore complex. *Bioessays.* 1997; 19: 787–92.
  36. **Perez-Terzic C, Pyle J, Jaconi M, et al.** Conformational states of the nuclear pore complex induced by depletion of nuclear Ca<sup>2+</sup> stores. *Science.* 1996; 273: 1875–7.
  37. **Bustamante JO, Michelette ERF, Geibel JP, et al.** Calcium, ATP and nuclear pore channel gating. *Pflugers Arch.* 2000; 439: 433–44.
  38. **Keminer O, Peters R.** Permeability of single nuclear pores. *Biophys J.* 1999; 77: 217–28.
  39. **Mazzanti M, Bustamante JO, Oberleithner H.** Electrical dimension of the nuclear envelope. *Physiol Rev.* 2001; 1: 1–19.
  40. **Shahin V, Danker T, Enss K, et al.** Evidence for Ca<sup>2+</sup>- and ATP-sensitive peripheral channels in nuclear pore complexes. *FASEB J.* 2001; 15: 1895–901.
  41. **Jans DA.** The regulation of protein transport to the nucleus by phosphorylation. *Biochem J.* 1995; 311: 705–16.
  42. **Jans DA, Hübner S.** Regulation of protein transport to the nucleus: central role of phosphorylation. *Physiol Rev.* 1996; 76: 651–85.
  43. **Kehlenbach RH, Gerace L.** Phosphorylation of the nuclear transport machinery down-regulates nuclear protein import *in vitro*. *J Biol Chem.* 2000; 275: 17848–56.
  44. **Favreau C, Worman HJ, Wozniak RW, et al.** Cell cycle-dependent phosphorylation of nucleoporins and nuclear pore membrane protein gp210. *Biochemistry.* 1996; 35: 8035–44.
  45. **Macaulay C, Meier E, Forbes DJ.** Differential mitotic phosphorylation of proteins of the nuclear pore complex. *J Biol Chem.* 1995; 270: 254–62.
  46. **Mishra K, Parnaik VK.** Essential role of phosphorylation in nuclear transport. *Exp Cell Res.* 1995; 216: 124–34.
  47. **Chahine MN, Blackwood DP, Dibrov E, et al.** Oxidized LDL affects smooth muscle cell growth through MAPK-mediated actions on nuclear protein import. *J Mol Cell Cardiol.* 2009; 46: 431–41.
  48. **Czubryt MP, Austria JA, Pierce GN.** Hydrogen peroxide inhibition of nuclear import is mediated by the mitogen-activated protein kinase, ERK-2. *J Cell Biol.* 2000; 148: 7–15.
  49. **Richard MN, Deniset JF, Kneesh AL, et al.** Mechanical stretching stimulates smooth muscle cell growth, nuclear protein import, and nuclear pore expression through mitogen-activated protein kinase activation. *J Biol Chem.* 2007; 282: 23081–8.
  50. **Faustino RS, Cheung P, Richard MN, et al.** Ceramide regulation of nuclear protein import. *J Lipid Res.* 2008; 49: 654–62.
  51. **Faustino RS, Stronger LN, Richard MN, et al.** RanGAP-mediated nuclear protein import in vascular smooth muscle cells is augmented by lysophosphatidylcholine. *Mol Pharmacol.* 2007; 71: 438–45.
  52. **Gilchrist JSC, Pierce GN.** Identification and purification of a calcium-binding protein in hepatic nuclear membranes. *J Biol Chem.* 1993; 268: 4291–9.
  53. **Berrios M.** Isolation and characterization of karyoskeletal protein-enriched fractions from vertebrate livers. In: Berrios M, editor. *Methods in cell biology: nuclear structure and function.* San Diego: Academic Press; 1998. pp. 3–22.
  54. **Zettler ME, Prociuk MA, Austria JA, et al.** OxLDL stimulates cell proliferation through a general induction of cell cycle proteins. *Am J Physiol Heart Circ Physiol.* 2003; 284: H644–53.
  55. **Czubryt MP, Ramjiawan B, Gilchrist JSC, et al.** The presence and partitioning of calcium binding proteins in hepatic and cardiac nuclei. *J Mol Cell Cardiol.* 1996; 28: 455–65.
  56. **Pang L, Sawada T, Decker SJ, et al.** Inhibition of MAP kinase kinase blocks the differentiation of PC-12 cells induced by nerve growth factor. *J Biol Chem.* 1995; 270: 13585–8.
  57. **Garnovskaya MN, Mukhin YV, Vlasova TM, et al.** Mitogen-induced rapid phosphorylation of serine 795 of the retinoblastoma gene product in vascular smooth muscle cells involves ERK activation. *J Biol Chem.* 2004; 279: 24899–905.
  58. **Nemoto S, Xiang J, Huang S, et al.** Induction of apoptosis by SB202190 through inhibition of p38beta mitogen-activated protein kinase. *J Biol Chem.* 1998; 273: 16415–20.

59. **Faustino RS, Czubryt MP, Pierce GN.** Determining influence of oxidants on nuclear transport using digitonin-permeabilized cell assay. *Meth Enzymol.* 2002; 352: 123–34.
60. **Matunis MJ.** Isolation and fractionation of rat liver nuclear envelopes and nuclear pore complexes. *Methods.* 2006; 39: 277–83.
61. **Levitan IB.** Modulation of ion channels by protein phosphorylation and dephosphorylation. *Annu Rev Physiol.* 1994; 56: 193–212.
62. **Light P.** Regulation of ATP-sensitive potassium channels by phosphorylation. *Biochim Biophys Acta.* 1996; 1286: 65–73.
63. **Qu Y, Rogers JC, Tanada TN, et al.** Phosphorylation of S1505 in the cardiac Na<sup>+</sup> channel inactivation gate is required for modulation by protein kinase C. *J Gen Physiol.* 1996; 108: 375–9.
64. **Faustino RS, Rousseau DC, Landry MN, et al.** Effects of mitogen-activated protein kinases on nuclear protein import. *Can J Physiol Pharmacol.* 2006; 84: 469–75.
65. **Kosako H, Yamaguchi N, Aranami C, et al.** Phosphoproteomics reveals new ERK MAP kinase targets and links ERK to nucleoporin-mediated nuclear transport. *Nat Struct Mol Biol.* 2009; 16: 1026–35.
66. **Ahn NG.** PORE-ing over ERK substrates. *Nat Struct Mol Biol.* 2009; 16: 1004–5.
67. **Gerasimenko OV, Gerasimenko JV, Tepikin AV, et al.** Calcium transport pathways in the nucleus. *Pflugers Arch.* 1996; 432: 1–6.
68. **Santella L, Carafoli E.** Calcium signaling in the cell nucleus. *FASEB J.* 1997; 11: 1091–109.
69. **Wang H, Clapham DE.** Conformational changes of the in situ nuclear pore complex. *Biophys J.* 1999; 77: 241–7.
70. **Khokhlatchev AV, Canagarajah B, Wilsbacher J, et al.** Phosphorylation of the MAP kinase ERK2 promotes its homodimerization and nuclear translocation. *Cell.* 1998; 93: 605–15.
71. **Shukla N, Rowe D, Hinton J, et al.** Calcium and the replication of human vascular smooth muscle cells: studies on the activation and translocation of extracellular signal regulated kinase (ERK) and cyclin D1 expression. *Eur J Pharmacol.* 2005; 509: 21–30.
72. **Caunt CJ, Rivers CA, Conway-Campbell BL, et al.** Epidermal growth factor receptor and protein kinase C signaling to ERK2: spatiotemporal regulation of ERK2 by dual specificity phosphatases. *J Biol Chem.* 2008; 283: 6241–52.
73. **Li M, Liu Y, Dutt P, et al.** Inhibition of serotonin-induced mitogenesis, migration, and ERK MAPK nuclear translocation in vascular smooth muscle cells by atorvastatin. *Am J Physiol Lung Cell Mol Physiol.* 2007; 293: L463–71.
74. **Hai CM, Gu Z.** Caldesmon phosphorylation in actin cytoskeletal remodeling. *Eur J Cell Biol.* 2006; 85: 305–9.
75. **Kordowska J, Huang R, Wang CL.** Phosphorylation of caldesmon during smooth muscle contraction and cell migration or proliferation. *J Biomed Sci.* 2006; 13: 159–72.
76. **Wang B, Chen J, Santiago FS, et al.** Phosphorylation and acetylation of histone H3 and autoregulation by early growth response 1 mediate interleukin 1(β) induction of early growth response 1 transcription. *Arterioscler Thromb Vasc Biol.* 2009; 30: 536–45.
77. **Fernandez-Martinez J, Rout MP.** Nuclear pore complex biogenesis. *Curr Opin Cell Biol.* 2009; 21: 603–12.
78. **Capelson M, Hetzer MW.** The role of nuclear pores in gene regulation, development and disease. *EMBO Rep.* 2009; 10: 697–705.
79. **Xylourgidis N, Fornerod M.** Acting out of character: regulatory roles of nuclear pore complex proteins. *Dev Cell.* 2009; 17: 617–25.